❒   18

Design of PI-neural controller for hybrid active power filter

Chau Minh Thuyen
Faculty of Electrical Engineering Technology, Industrial University of Ho Chi Minh City, Viet Nam

Article Info	ABSTRACT
	This paper aims to design a control method using an adaptive controller for Hybrid Active Power Filter. The controller of designed method includes a traditional discrete Proportional Integral controller and a neural regulator. The neural regulator is used to estimate the nonlinear model of Hybrid Active Power Filter and predict an output value in the future to adjust the parameters of the traditional discrete Proportional Integral controller according to the change of load. Compared to the control method using a conventional Proportional Integral controller, the proposed controller shows the advantages of smaller compensation error and smaller total harmonic distortion and able to online control very well. The simulations have verified the effectiveness of proposed controller.

Corresponding Author:

Chau Minh Thuyen,
Faculty of Electrical Engineering Technology,
Industrial University of Ho Chi Minh City, Viet Nam.
Email: chauminhthuyen@iuh.edu.vn

1.   INTRODUCTION

The Hybrid Active Power Filter (HAPF) is considered as an effective solution to improve power quality on electrical systems. It is very effective in reducing harmonics and reactive power compensation with a relatively low capacity of Active Power Filter [1-7]. However, the performance of HAPF depends on many factors, such as: the used controller, control strategy, harmonic detection method, the exact determination of the circuit parameters, etc. In which, the controller plays a very important role, it affects the accuracy of the HAPF system.

The controllers that have been used for control HAPF can be summarized as follows: the Hysteresis controller is characterized by its simplicity and fast response, but its disadvantage is that it depends on a widely varying switching frequency [8, 9]. The conventional Proportional Integral (PI) controller has many advantages such as a simple structure and ease of use [10, 11]. However, the K_P and K_I parameters are fixed during the whole control process. Therefore, with fast variable nonlinear loads, the dynamic response of the PI controller is not good. With the fuzzy logic controllers, using the Mamdani Fuzzy Inference System is the most popular. It is conceptually easy to understand, flexible and it can be combined with conventional control techniques [12-17]. However, the input-output memberships are fixed and cannot be learned during the whole control process and its parameters depends on experience. To improve the disadvantages of the fuzzy controller, another controller used for HAPF is Adaptive Neural Fuzzy Inference System (ANFIS) controller [18, 19]. The ANFIS controller uses techniques such as hybrid or back propagation learning rules to determine the input membership functions. Flowing that, the input membership functions after learning will give the desired results in the output. However, the ANFIS controller also has some drawbacks such as the fact that: it has a single output, all of the output membership functions must be the same type (they must be either be linear or constant), different rules cannot share the same output membership function, have unity weight for each rule, based on the given learning data sets.

Neural controllers are also used for control HAPF [20-25], the advantage of this controller is the self-learning ability of neural networks, but its disadvantage is able to respond slowly and need to have a sample data set. From the above analysis, this paper presents a discrete PI-neural controller for HAPF, which consists of two controller units: a traditional discrete PI controller and a neural adjustor. The neural network model used in this paper is an identification and predictive neural network. First, neural networks will identify the nonlinear model of HAPF and then predict an output value in future. This predictive output value will be used to online regulate parameters of the traditional PI controller. Therefore, the proposed controller can improve the performance of the traditional PI controller and it has the ability to control online very well and is very suitable for nonlinear controls.

This paper is organized as follows: Section 1 gives an introduction of the former research on the HAPF. Control block diagram for HAPF is highlighted in Section 2. Section 3 represents the proposed controller for the HAPF. Simulation results are presented in Section 4, and Section 5 draws some conclusions.

2. CONTROL BLOCK DIAGRAM FOR HAPF

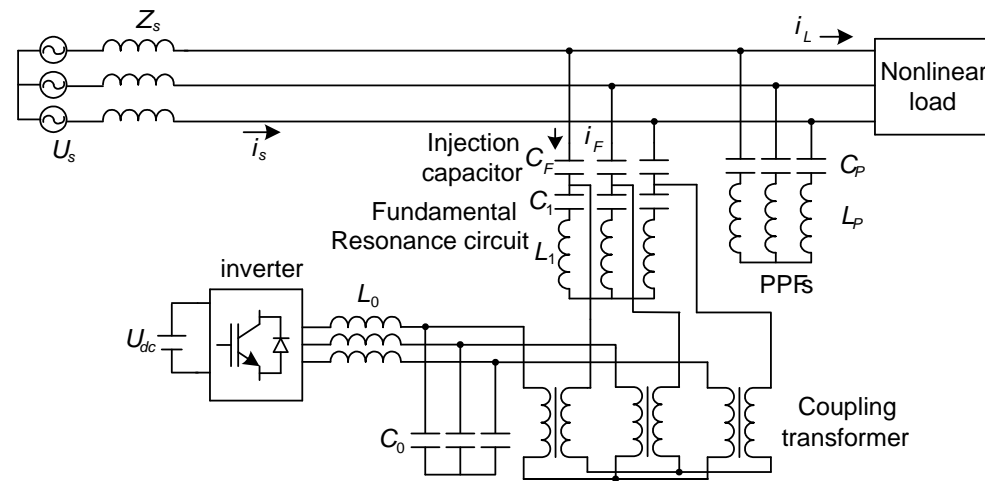The topology of the HAPF is proposed as shown in Figure 1.

Figure 1. Topology of the HAPF

where: U_s and Z_s are the supply voltage and the equivalent impedance of the grid, respectively. C_F, C_1, L_1, C_P, L_P, L_0, and C_0 are the injection capacitor, the fundamental resonance capacitor, the fundamental resonance inductor, the PPF capacitor, the PPF inductor, the output filter inductor and the output filter capacitor, respectively.

A single-phase equivalent circuit of the HAPF is shown in Figure 2.
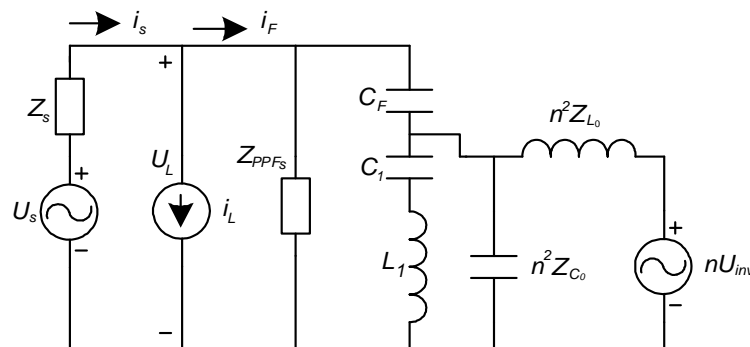

Figure 2. Single-phase equivalent circuit of HAPF

A single-phase equivalent circuit when only the voltage source inverter U_{inv} is considered (U_s =0; i_L =0) is shown in Figure 3.
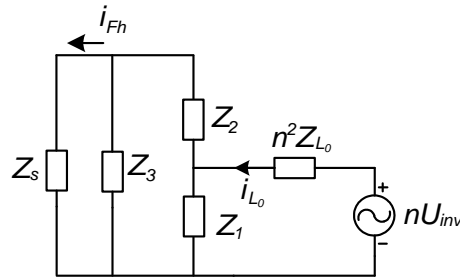

Figure 3. Single-phase equivalent circuit when only the U_{inv} is considered

Where:

$$\begin{cases} Z_s = R_s + L_s s \\ Z_1 = Z_{L_1 C_1} // n^2 Z_{C0} \\ Z_2 = \dfrac{1}{C_F s} \\ Z_{L0} = R_0 + L_0 s \\ Z_3 = Z_{PPFs} \end{cases} \tag{1}$$

From Figure 3, the harmonic current injection into the grid by the HAPF can be calculated:

$$i_{Fh} = \frac{nU_{inv}.Z_1.Z_3}{n^2 Z_{L0}[Z_3(Z_1 + Z_2) + Z_s(Z_1 + Z_2 + Z_3)] + Z_1(Z_2 Z_s + Z_2 Z_3 + Z_3 Z_s)} \tag{2}$$

equation (2) indicates that, compensation harmonic current is determined by the voltage source inverter U_{inv} and the response of the output circuit $G_{out}(s)$, with $G_{out}(s)$ is the transfer function of the compensation harmonic current i_{Fh} to the inverter output voltage U_{inv}.

$$G_{out}(s) = \frac{i_{Fh}}{U_{inv}} = \frac{nZ_1.Z_3}{n^2 Z_{L0}[Z_3(Z_1 + Z_2) + Z_s(Z_1 + Z_2 + Z_3)] + Z_1(Z_2 Z_s + Z_2 Z_3 + Z_3 Z_s)} \tag{3}$$

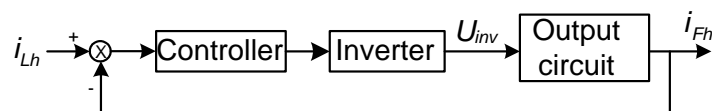The control strategy based on load harmonic current detection [19] is shown in Figure 4.

Figure 4. Control strategy based on load harmonic current detection

3. DESIGN OF DISCRETE PI-NEURAL CONTROLLER FOR HAPF

From the control block diagram shown in Figure 4, we can build control block diagram for HAPF using PI-neural controller as shown in Figure 5.
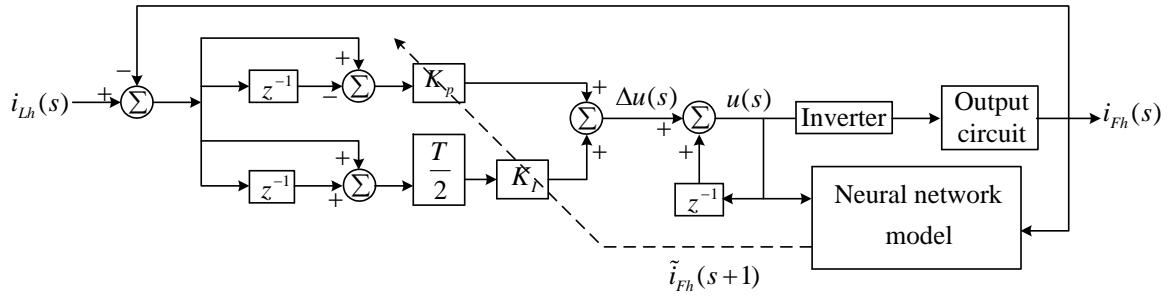
Figure 5. Control block diagram for HAPF using discrte PI-neural controller

A typical discrete-time PI controller can be expressed as:

$$u(s) = u(s-1) + \Delta u(s)$$
$$= u(s-1) + K_P[(e(s) - e(s-1)] + \frac{K_I T}{2}[(e(s) + e(s-1)] \tag{4}$$

where $u(s)$ is the control effort at time s, K_P and K_I are proportional and integral gains, respectively. T is the sampling period, $e(s)$ is the tracking error defined as $e(s)=i_{Lh}(s)-i_{Fh}(s)$, $i_{Lh}(s)$ is the desired plant output, $i_{Fh}(s)$ is the actual plant output. The *PI* controller can also be expressed in the following form:

$$\Delta u(s) = K_P e_P(s) + K_I e_I(s) \tag{5}$$

where:

$$e_P(s) = e(s) - e(s-1)$$
$$e_I(s) = \frac{T}{2}[e(s) + e(s-1)]$$

The neural network model assumes two functions: the first function is to identify the nonlinear model of HAPF and the second function is to predict an output value at the time $(s + 1)$. The neural network model used here is a feed-forward neural network and the back-propagation algorithm is used to train the weights. The inputs of neural networks are $u(s)$ and $i_{Fh}(s)$.

The output of the HAPF nonlinear model is a function of the form:

$$i_{Fh}(s) = f[i_{Fh}(s-1), i_{Fh}(s-2), \dots i_{Fh}(s-n+1), u(s-1), u(s-m+1)] \tag{6}$$

where $i_{Fh}(s)$ is the scalar output of the system, $u(s)$ is the scalar input to the system, n and m are the output and the input orders respectively, $f[\dots]$ is the unknown nonlinear function to be estimated by a Neural Network.
The output of neural network model is a function of the form:

$$\tilde{i}_{Fh}(s) = \tilde{f}[i_{Fh}(s-1), i_{Fh}(s-2), \dots i_{Fh}(s-n+1), u(s-1), u(s-m+1)] \tag{7}$$

where $\tilde{i}_{Fh}(s)$ is the output of the neural model and $\tilde{f}$ is the estimate of f.
Since then we have the predictive output of the neural network at the time $(s + 1)$ will be:

$$\tilde{i}_{Fh}(s+1) = \tilde{f}[i_{Fh}(s), i_{Fh}(s-1), \dots i_{Fh}(s-n+1), u(s), u(s-1), u(s-m+1)] \tag{8}$$

The weights of the neural model are adjusted to minimize the cost function given by:

$$E = \frac{1}{2}\left[i_{Lh}(s+1) - \tilde{i}_{Fh}(s+1)\right] \tag{9}$$

The weight tuning update for the gains using descent method is given by:

$$\Delta K_{P,I}(s) = -\alpha \frac{\partial E}{\partial K_{P,I}} + \beta \Delta K_{P,I}(s-1) \tag{10}$$

where α is the learning rate and β is the momentum rate.

The derivatives in equation (10) are computed as:

$$\frac{\partial E}{\partial K_P} = \frac{\partial E}{\partial \tilde{i}_{Fh}(s)} \frac{\partial \tilde{i}_{Fh}(s)}{\partial u(s)} \frac{\partial u(s)}{\partial K_P} = -\left(i_{Lh}(s) - \tilde{i}_{Fh}(s)\right) \frac{\partial \tilde{i}_{Fh}(s)}{\partial u(s)} e_P(s) \tag{11}$$

$$\frac{\partial E}{\partial K_I} = \frac{\partial E}{\partial \tilde{i}_{Fh}(s)} \frac{\partial \tilde{i}_{Fh}(s)}{\partial u(s)} \frac{\partial u(s)}{\partial K_I} = -\left(i_{Lh}(s) - \tilde{i}_{Fh}(s)\right) \frac{\partial \tilde{i}_{Fh}(s)}{\partial u(s)} e_I(s) \tag{12}$$

As the hidden and output neuron functions were defined by the logistic sigmoid function then $\frac{\partial \tilde{i}_{Fh}(s)}{\partial u(s)}$ is expressed as:

$$\frac{\partial \tilde{i}_{Fh}(s)}{\partial u(s)} = \tilde{i}_{Fh}(s)\left(1 - \tilde{i}_{Fh}(s)\right) \sum_j W_j^m O_j^m \left(1 - O_j^m\right) W_{1j}^m \tag{13}$$

O_j^m is the output of jth neuron in the hidden layer of the neural network, W_{1j}^m and W_j^m are the weights of the neural network from the input neurons to intermediate layer, and from the intermediate layer to the output.

4. SIMULATION RESULTS AND DISCUSSION

Simulation results of a 10kV-50Hz HAPF system have been made with the MATLAB software. The system parameters are listed in Table 1. The nonlinear load is established by four harmonic current sources 5th, 7th, 11th and 13th. PPFs are passive power filters, they are 11th and 13th turned filters. The DC-bus voltage is 600V.

Table 1. Simulation parameters of HAPF

	L(mH)	C(μF)	Q
Output filter	0.2	60	
11th turned filter	1.77	49.75	50
13th turned filter	1.37	44.76	50
Fundamental resonance circuit	14.75	690	
Injection circuit		19.65	

The simulation results with the traditional discrete PI controller ($K_P = 10$, $K_I = 0.1$) are shown in Figure 6. The simulation results with the traditional discrete PI controller in steady-state shown in Figure 7. $u_s(V)$, $i_L(A)$, $i_s(A)$ and $error(A)$ represents the source voltage, load current, supply current and error of compensation of phase A, respectively.

During the period from 0s to 0.1s, only passive power filters close to the system. At time t = 0.1s, APF is closed to the system and at the time t = 0.6s the load is changed.

During the period from 0.5s to 0.6s, the total harmonic distortion (THD) of the load current is 15.75%, the THD of the supply current decreases to 2.66% from 15.75%, the compensation error decreases to ± 10A from ± 100A. Figure 8 shows the THD of the load current before the load is changed. Figure 9 shows the THD of the supply current before the load is changed.

During the period from 0.9s to 1.0s, THD of the load current is 21%, THD of the supply current decreases to 3.75% from 21%, the compensation error increases to ± 18A from ± 10A. Figure 10 shows the THD of the load current after the load is changed. Figure 11 shows the THD of the supply current after the load is changed.

The simulation results with the proposed controller (initial parameters of the discrete PI controller are $K_P = 10$, $K_I = 0.1$) are shown in Figure 12. The simulation results with the proposed controller in steady-state are shown in Figure 13.
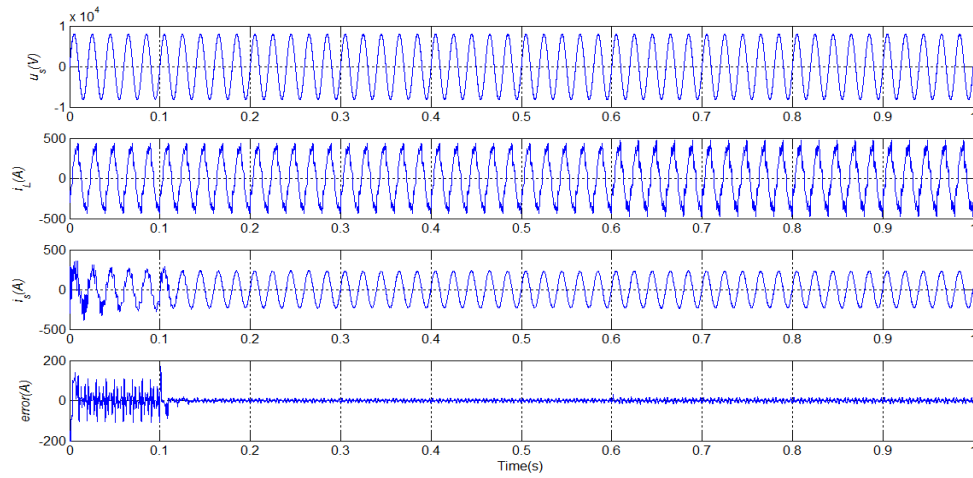

Figure 6. Dynamic response of HAPF with traditional discrete PI controller
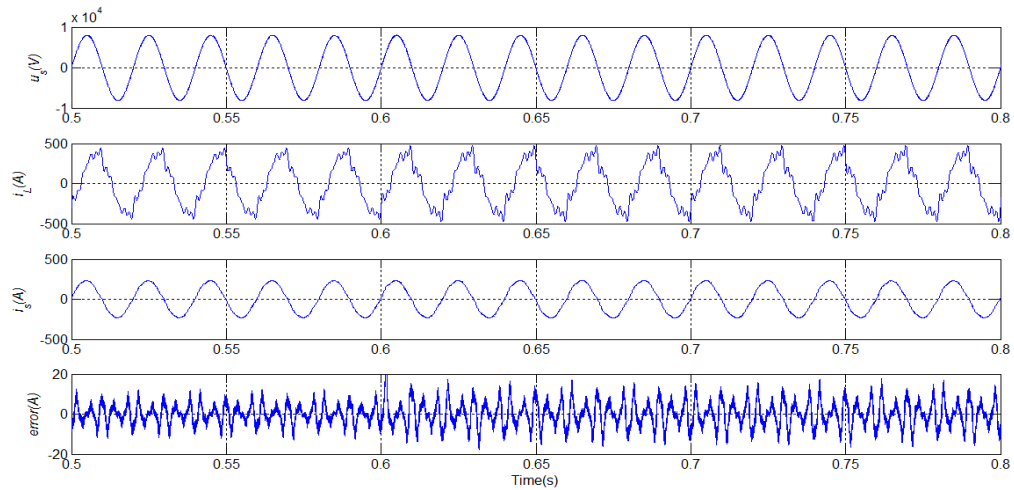

Figure 7. Simulation results with traditional discrete PI controller in steady-state
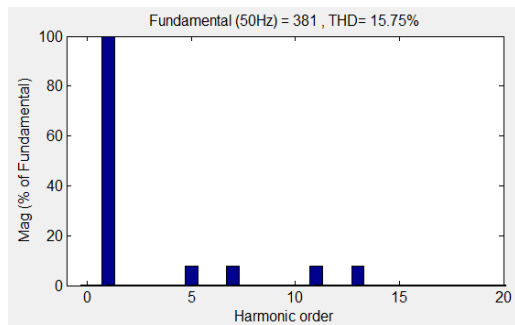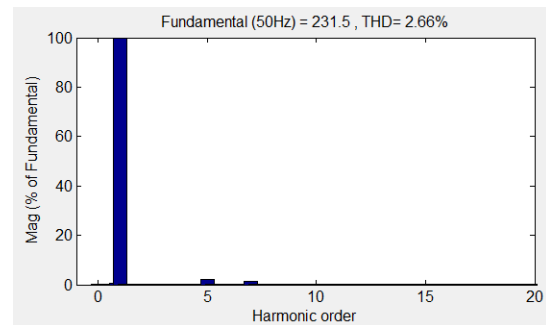

Figure 8. THD of i_L before the load is changed

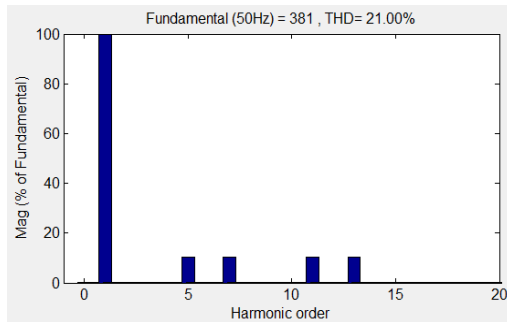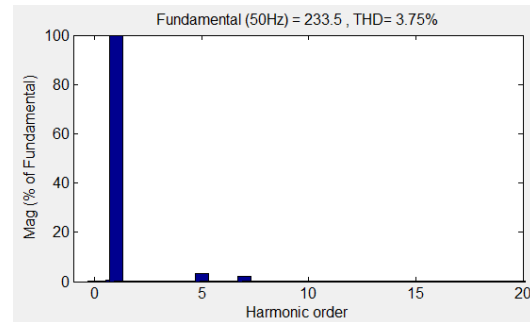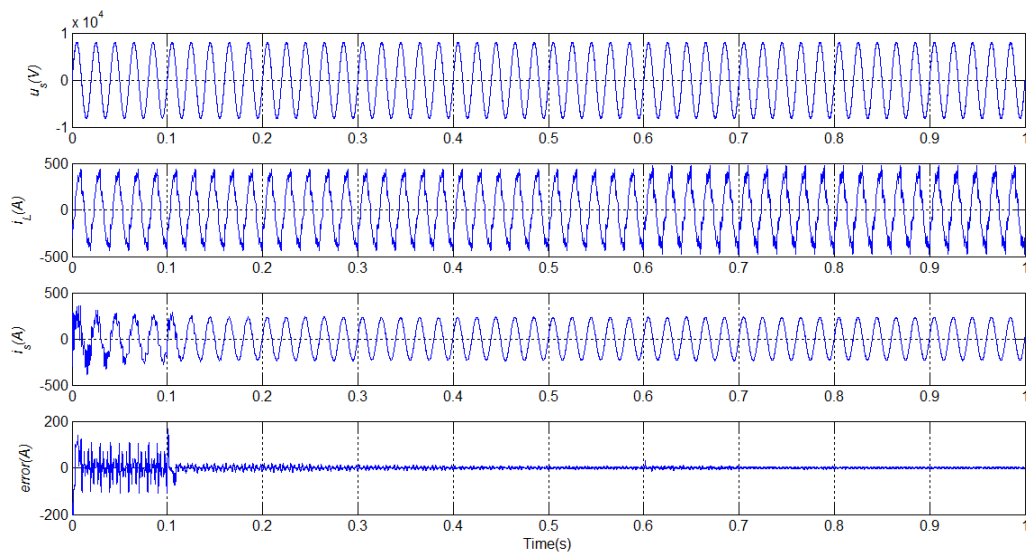Figure 9. THD of i_s before the load is changed

Figure 10. THD of the i_L after the load is changed   Figure 11. THD of the i_s after the load is changed

Figure 12. Dynamic response of HAPF with the proposed controller

During the period from 0.5s to 0.6s, THD of the load current is 15.75%, THD of the supply current decreases to 1.2% from 15.75%, the compensation error decreases to ± 5A from ± 100A. Figure 14 shows the THD of the supply current before the load is changed.

During the period from 0.9s to 1.0s, THD of the load current is 21%, THD of the supply current decreases to 1.09% from 21%, the compensation error is ± 5A. Figure 15 shows the THD of the supply current after the load is changed.

A comparison table of the *THD* i_s, *cosφ* and *error* in the steady-state of two controllers is summarized in Table 2.

Table 2. Comparison of the *THD* i_s, *cosφ* and *error* in the steady-state of two controllers

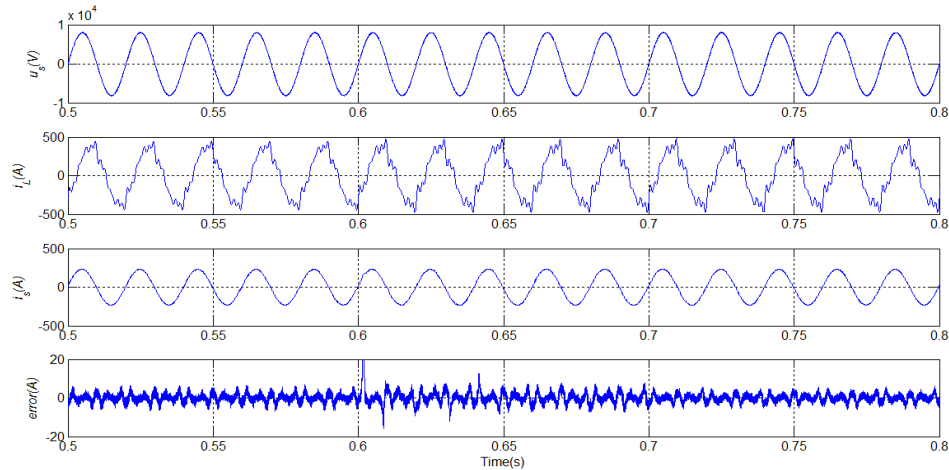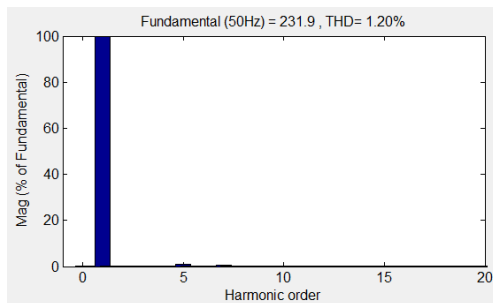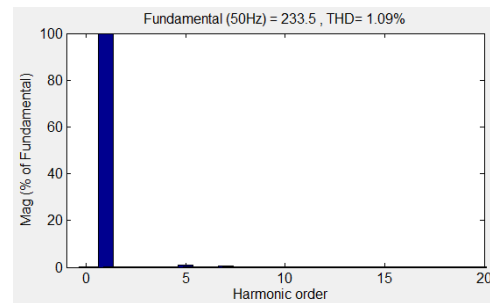|	0.5s÷0.6s			0.9s÷1.0s		
	THD i_s (%)	cosφ	error (A)	THD i_s (%)	cosφ	error (A)
Before compensation	15.75	0.64	±100	21	0.64	±100
After compensation with the traditional PI controller	2.66	0.984	±10	3.75	0.982	±18
After compensation with the proposed controller	1.2	0.986	±5	1.09	0.985	±5

Figure 13. Simulation results with the proposed controller in steady-state

Figure 14. THD of i_s before load is changed

Figure 15. THD of i_s after the load is changed

From the above simulation results we can see that: the control method using discrete PI-neural controller is more efficient than the control method using a traditional discrete PI controller in reducing the THD of the supply current and reducing the compensation error in steady-state. In particular, the PI-neural controller has the ability to online control very well.

5. CONCLUSION

This paper has built a discrete PI-neural controller for Hybrid Active Power Filter. Compared to the control method using the traditional PI controller, the simulation results have demonstrated that: the control method using a discrete PI-neural controller has a compensation error in steady-state and total harmonic distortion of the supply current is smaller. In addition, the controller is also capable of controlling online very well, especially the ability to adapt each time there is a change of load. It is also useful and applicable to other Hybrid Active Power Filters, especially for nonlinear control systems.

REFERENCES

[1]   Z Shuai, *et al.*, "New control method of injection-type hybrid active power filter," *IET Power Electronics*, vol. 4, pp. 1051-1057, 2011.
[2]   Minh Thuyen Chau, "Generalized current delay compensation on hybrid Active power filter," *ICIC express letters,* vol. 11, pp. 1409-1415, 2017.
[3]   Chau Minh Thuyen, "Improved p-q Harmonic Detection Method for Hybrid Active Power Filter," *International Journal of Electrical and Computer Engineering (IJECE)*, vol. 8, pp. 2910– 2919, 2018.
[4]   Ibrahim Alhamrouni, et al., "Modeling of Micro-grid with the consideration of total harmonic distortion analysis," *Indonesian Journal of Electrical Engineering and Computer Science (IJEECS)*, vol. 15, pp. 581-592, 2019.
[5]   A Luo, *et al.*, "Design Considerations for Maintaining DC-Side Voltage of Hybrid Active Power Filter With Injection Circuit," *IEEE Transactions on Power Electronics*, vol. 24, pp. 75-84, 2009.

[6]   Y K Latha, *et al.*, "Control Strategy for Three Phase Shunt Active Power Filter with Minimum Current Measurements," *International Journal of Electrical and Computer Engineering (IJECE)*, vol. 1, pp. 31-42, 2011.

[7]   F Ruixiang, *et al.*, "Parameter design and application research of shunt hybrid active power filter," *Proc. CSEE*. 2006, vol. 26, pp. 106–111, 2006.

[8]   Y Panda and A K Suresh, "Real-Time Implementation of Adaptive Fuzzy Hysteresis-Band Current Control Technique for Shunt Active Power Filter," *IET Power Electronics*, vol. 5, pp. 1188–1195, 2012.

[9]   A Hamadi, *et al.*, "Comparison of Fuzzy logic and Proportional Integral Controller of Voltage Source Active Filter Compensating Current Harmonics and Power Factor," *IEEE International Conference on Industrial Technology (ICIT)*, 2001, pp. 645-650.

[10] Y Chen, *et al.*, "Fuzzy logic based auto-modulation of parameters PI control for active power filter," In*telligent Control and Automation, WCICA*. 2008, pp. 5228-5232.

[11] Pankaj Gakhar and Manoj Gupta, "A novel control strategy for power quality improvement in grid-connected solar photovoltaic system," *Indonesian Journal of Electrical Engineering and Computer Science (IJEECS)*, vol. 15, pp. 1264-1272, 2019.

[12] C Wei, *et al.*, "Method of Event Detection Based on Dynamic Hybrid Fuzzy Logic System," *International Conference on Intelligent Computation Technology and Automation*. 2010, pp. 661-663.

[13] An Luo, *et al.*, "Development of Hybrid Active Power Filter Based on the Adaptive Fuzzy Dividing Frequency-Control Method," *IEEE Transactions on Power Delivery*, vol. 24, pp. 424-432, 2009.

[14] Ahmed A Helal, *et al.*, "Fuzzy Logic Controller Shunt Active Power Filter for Three-phase Four-wire systems with Balanced and Unbalanced Loads," *World Academy of Science, Engineering and Technology*, vol. 5, pp. 621-626, 2009.

[15] C N Bhende, *et al.*, "TS-Fuzzy-Controlled Active Power Filter for Load Compensation," *IEEE Transactions on Power Delivery*, vol. 21, pp. 1459–1465, 2006.

[16] S Kerrouche and F Krim, "Three-phase Active Power Filter Based on Fuzzy logic controller," *International Journal of Sciences and Techniques of Automatic control & computer engineering IJ-STA*, vol. 3, pp. 942-955, 2009.

[17] O Karasakal, *et al.*, "Online Rule Weighting of Fuzzy PID Controllers," *IEEE International Conference on System Man and Cybernetics (SMC)*, 2010, pp. 1741-1747.

[18] K Çağatay Bayındır, *et al.*, "Hierarchical neuro-fuzzy current control for a shunt active power filter," *Neural Computing and Applications*, vol. 15, pp. 223-238, 2006.

[19] Minh Thuyen Chau, "Adaptive Current Control Method for Hybrid Active Power Filter," *Journal of Electrical Engineering*, vol. 67, pp. 343–350, 2016.

[20] Aravind Ravikumar *et al.*, "Performance Enhancement of a Series Active Power Filter using Kalman Filter based Neural Network Control Strategy," *International Conference on Advances in Computing, Communications and Informatics* (ICACCI), 2018, pp. 1702-1706.

[21] Juntao Fei and Di Cao, "Adaptive Fractional Terminal Sliding Mode Controller for Active Power Filter Using Fuzzy-Neural-Network," *10th International Conference on Knowledge and Systems Engineering (KSE)*, 2018, pp. 118-122.

[22] Juntao Fei,*et al.*, "Adaptive Fuzzy-Neural-Network Control of Active Power Filter Using Fuzzy Backstepping Approach," *First International Symposium on Instrumentation, Control, Artificial Intelligence, and Robotics* (ICA-SYMP), 2019, pp. 1-4.

[23] Kishore Kumar Pedapenki, *et al.*, "Application of neural networks in power quality," *International Conference on Soft Computing Techniques and Implementations* (ICSCTI), 2015, pp. 116-119.

[24] Mohd Hafizul Afifi Abdullah1, et al., "Evolving spiking neural networks methods for classification problem: a case study in flood events risk assessment," *Indonesian Journal of Electrical Engineering and Computer Science (IJEECS)*, vol. 16, pp. 222-229, 2019.

[25] C Madtharad and S Premrudeepreechachrn, "Active power filter for three-phase four-wire electric systems using neural networks," *Elect. Power Syst. Res*, vol. 60, pp. 179-192, 2002.

BIOGRAPHY OF AUTHOR

Chau Minh Thuyen was born in Binh Dinh, Vietnam, on June 6, 1977. He received his B.S. and M.S. from the Da Nang University of Technology, Da Nang, Viet Nam, and the University of Technical Education Ho Chi Minh City, Ho Chi Minh City, Viet Nam, in 2001 and 2005, respectively, and Ph.D. from Hunan University, China, in 2012. Since 2004, he has been a Lecturer at Industrial University of Ho Chí Minh City, Viet Nam. His current research includes power electronics, electric power savings, reactive power compensation, and active power filters.